XPS and ESR of $SnSe_2$–1%$P\{CoCp_2\}_{0.36}$

D. A. Cleary*

Department of Chemistry, Washington State University, Pullman, Washington 99164-4630

D. R. Baer

Molecular Sciences Research Center, Pacific Northwest Laboratory, Richland, Washington 99352

Received July 9, 1991. Revised Manuscript Received October 1, 1991

We have measured the Co $2p_{3/2}$ X-ray photoelectron (XPS) spectrum of $SnSe_2$–1%$P\{CoCp_2\}_{0.36}$ as a function of time and have found that the Co $2p_{3/2}$ profile changes with time. This indicates that $SnSe_2$-1%$P\{CoCp_2\}_{0.36}$ undergoes radiation damage as a result of X-ray exposure. Consideration of this damage is important when attempting to use XPS as a measure of the Co^{2+}/Co^{3+} ratio is this material. Our X-band ESR spectra of $SnSe_2$–1%$P\{CoCp_2\}_{0.36}$ are consistent with the presence of neutral cobaltocene in this material. Quantitative agreement between the XPS and ESR results is achieved when the temporal change in the XPS line shape is modeled using second-order kinetics.

Introduction

Superconductivity is known to occur in several of the layered transition-metal dichalcogenides, MX_2, where M is an early transition metal and X is S, Se, or Te.[1] An important discovery in this field came in 1970 when Gamble et al. reported the dramatic increase in T_c of TaS_2 when the TaS_2 was intercalated with pyridine to produce $TaS_2\{pyridine\}_{1/2}$.[2] The T_c of pure TaS_2 is 0.7 K, whereas the pyridine intercalated material has a T_c of 3.5 K. The inclusion of an organic molecule, pyridine, into an inorganic host, TaS_2, raised the critical temperature by a factor of 5. Recently, Formstone et al. have reported superconductivity in $SnSe_2$–1%P when it is intercalated with cobaltocene ($CoCp_2$ where Cp ≡ $C_5H_5^-$) to produce $SnSe_2$–1%$P\{CoCp_2\}_{0.33}$.[3] This is a remarkable finding given that neither $SnSe_2$ nor $SnSe_2$–1%P have been shown to be intrinsic superconductors. In fact, $SnSe_2$, a layered post-transition-metal dichalcogenide, is a rather wide (1 eV) indirect bandgap semiconductor.[4] The phosphorus is added to pure $SnSe_2$ to enhance its low electrical conductivity. Both the pure and phosphorus doped $SnSe_2$ are n-type semiconductors.[3]

In addition to its intercalation chemistry with transition- and post-transtion-metal dichalcogenides, cobaltocene undergoes intercalation reactions into transition-metal phosphorus chalcogenides, $M_2P_2X_6$, where M is a transition metal and X is sulfur or selenium.[5-10] An intriguing question regarding cobaltocene intercalation chemistry is what percentage of the intercalated cobaltocene molecules are oxidized upon intercalation. In the case of cobaltocene intercalation of TaS_2, the evidence (primarily magnetic susceptibility) strongly suggests that all of the intercalated cobaltocene molecules are oxidized to cobaltocenium, $CoCp_2^+$.[11] In contrast, our recent work using $Cd_2P_2S_6$ as the host lattice demonstrated that a significant (≈20%) amount of the intercalated cobaltocene can remain unoxidized, that is, neutral. Such a compound can be expressed as

$$Cd_2P_2S_6\{CoCp_2\}_{0.17}\{CoCp_2^+\}_{0.63}$$

where the reduced species must be some component of the $Cd_2P_2S_6$ lattice. In the $Cd_2P_2S_6$ study, the relative amounts of cobaltocene and cobaltocenium were determined using a combination of chemical analysis and quantitative ESR. (The cobaltocene is paramagnetic and the cobaltocenium is diamagnetic.) A mixture of neutral and oxidized cobaltocene was also proposed by Parkinson et al.[12] for the intercalation compound formed between cobaltocene and SnS_2. The resulting compound is written

$$(Sn^{4+}_{0.9}Sn^{2+}_{0.1})S_2\{CoCp_2\}_{0.1}\{CoCp_2^+\}_{0.2}$$

In this case, ^{119}Sn Mössbauer spectroscopy was used to determine the specific component of the SnS_2 which served as the oxidizing agent. A combination of ^{119}Sn Mössbauer, magnetic susceptibility, and X-ray photoelectron spectroscopy (XPS) was used to determine the relative amounts of cobaltocene and cobaltocenium in SnS_2. Their rationale for the mixture of $CoCp_2$ and $CoCp_2^+$ is that the redox potential of cobaltocene is close to the Fermi level of SnS_2. As SnS_2 is reduced by cobaltocene ($Sn^{+4} \rightarrow Sn^{+2}$), the Fermi level of the intercalated phase rises until it equals the redox potential of cobaltocene. At that point, there is no net driving force for further charge transfer, and subsequent intercalation involves only neutral cobaltocene molecules until steric effects prevent continued uptake. The net effect is the establishment of an equilibrium between oxidized cobaltocene and reduced SnS_2.

The important difference between TaS_2, where the cobaltocene is fully cationic, and SnS_2, where only some of the cobaltocene molecules are cationic, is the electron affinity, χ, of the host dichalcogenide. Ultraviolet photoelectron (UPS) measurements on TaS_2 and SnS_2 show that the electron affinity of TaS_2 is approximately 1 eV greater than that of SnS_2.[13,14] This is consistent with a

(1) Fong, C. Y.; Schluter, M. *Electrons and Phonons in Layered Crystal Structures*; Weiting, T. J., Schluter, M., Eds.; D. Reidel: Dordrecht, The Netherlands, 1979; p 145.
(2) Gamble, F. R.; Di Salvo, F. J.; Klemm, R. A.; Geballe, T. H. *Science* **1970**, *168*, 568.
(3) Formstone, C. A.; Fitzgerald, E. T.; O'Hare, D.; Cox, P. A.; Kurmoo, M.; Hodby, J. W.; Lillicrap, D.; Goss-Custard, M. *J. Chem. Soc., Chem. Commun.* **1990**, *6*, 501.
(4) Schülter, I. C.; Schülter, M. *Phys. Status Solidi B* **1973**, *57*, 145.
(5) Kim, K.; Liddle, D. J.; Cleary, D. A. *J. Phys. Chem.* **1990**, *94*, 3205.
(6) Kim, K.; Cleary, D. A. *J. Phys. Chem.* **1990**, *94*, 3816.
(7) Long, G. T.; Cleary, D. A. *J. Solid State Chem.* **1990**, *87*, 77.
(8) Cleary, D. A.; Francis, A. H. *J. Phys. Chem.* **1985**, *89*,
(9) Michalowicz, A.; Clement, R. *Inorg. Chem.* **1982**, *21*, 3872.
(10) Clement, R.; Audiere, J.-P.; Renard, J.-P. *Rev. Chim. Miner.* **1982**, *19*, 560.
(11) Gamble, F. R.; Thompson, A. H. *Solid State Commun.* **1978**, *27*, 379.
(12) O'Hare, D.; Jaegermann, W.; D. L. Williamson, D. L.; Ohuchi, F. S.; Parkinson, B. A. *Inorg. Chem.* **1988**, *27*, 1537.
(13) Shepard, F. R.; Williams, P. M.; *J. Phys. C: Solid State Phys.* **1974**, *7*, 4427.

0897-4756/92/2804-0112$03.00/0

higher degree of charge transfer between cobaltocene and TaS_2 versus cobaltocene and SnS_2. In determining the degree of charge transfer between cobaltocene and SnS_2 versus $SnSe_2$, the electron affinity again must be considered. In this case, the measured difference is small; χ = 4.2 eV for SnS_2 and 4.35 eV for $SnSe_2$.[14] Nonetheless, from this consideration alone, one would expect a higher degree of charge transfer between cobaltocene and $SnSe_2$ than between cobaltocene and SnS_2. The XPS and ESR results presented in this paper are consistent with that prediction. For quantitative agreement between the two techniques, however, the XPS results must be extrapolated to zero X-ray exposure time as discussed below.

The significance of the work presented in this paper is that it provides experimental results consistent with the mechanism put forward by Parkinson et al. At the same time, it highlights a pitfall in the use of XPS with intercalated materials and suggests that further study of the effect of X-ray irradiation on intercalated materials is required before XPS can be used as a diagnostic tool in the characterization of these materials.

Experimental Section

Preparation. Materials. All of the materials used were from commercial suppliers and used as received. Tin was in the form of 20 mesh granular and was supplied by Mallinckrodt. Selenium powder, 60 mesh, was supplied by Johnson Mathey Inc. (USA). Red phosphorus powder, amorphous, 100 mesh, was purchased from Alfa. Resublimed iodine crystals (used as transporting agent) were from Johnson Mathey Chemicals Ltd. (England). Anhydrous acetonitrile was obtained from Aldrich Chemical Co. Cobaltocene crystals were from Strem Chemical Co.

Synthesis. $SnSe_2$–1P% was prepared from the constituent elements using chemical vapor transport. Stoichiometric amounts of tin and selenium (4 g total) were ground together lightly to ensure complete mixing. Phosphorus (1 mol %; 0.0044 g) was added and ground as well. The sample was transferred to a quartz reaction tube, iodine crystals (0.217 g) were added, and the tube was sealed off under vacuum. The tube was placed in a horizontal tube furnace, and a temperature gradient established such that the cool crystal growing zone was at 610 °C. The hot zone of the tube was ≈640 °C. Within 1 day all of the material transports from the hot zone to the cool zone. The tube is opened, and the product crystals are recovered. Any iodine adhering to the crystals is sublimed off prior to opening the reaction tube. The intercalated phase was prepared by soaking several crystals of $SnSe_2$–1%P in a 0.1 M acetonitrile solution of cobaltocene for 21 days at 60 °C. The sample is prepared in a drybox because of the air sensitivity of cobaltocene. The reaction is run in a sealed Pyrex tube. At the conclusion of the reaction, the tube is opened in the drybox, and the crystals are rinsed with acetonitrile. Both before and after intercalation, the crystals are black, opaque, and lustrous.

Characterization. Surface Analysis. X-ray photoelectron spectroscopy, XPS, spectra were collected on a Perkin-Elmer Physical Electronics 560 (large double-pass cylindrical mirror analyzer (CMA)) system using a nonmonochromatic Mg Kα X-ray source. The binding energy scale was calibrated by adjusting the $3p_{3/2}$ and $2p_{3/2}$ photolines for clean copper to appear at 75.13 ± 0.02 and 932.67 ± 0.02 eV, respectively. Survey data were collected with a 100-eV pass energy, and multiplex data were collected at 25-eV pass energy. A 4-kV Ar ion beam was used for sputtering some of the specimens. The nominal sputter rate used to determine sputter damage was ≈36 Å/min, calibrated for SiO_2. The $SnSe_2$–1%$P\{CoCp_2\}_{0.36}$ specimens were prepared for analysis by opening fresh layers for analysis in the main vacuum system. This was accomplished by mounting a flat portion of the material on a specimen mount in the spectrometer. The outer surface of the specimen was then placed in contact with double sticky tape. When the tape was pulled from the surface, a fresh layer of material was exposed. Because of the way the specimen was mounted, there may be some charging that has not been corrected for in the data.

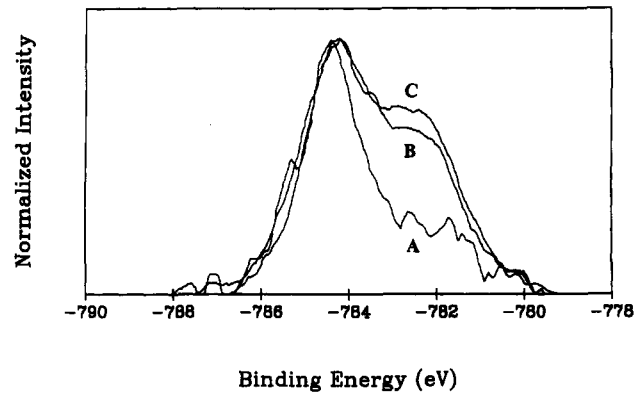

Figure 1. Co $2p_{3/2}$ XPS photoline from $SnSe_2$–1%$P\{CoCp_2\}_{0.36}$. Spectra are from X-ray exposure times of (A) 15 min, (B) 120 min, and (C) 300 min.

Electron Spin Resonance. X-band (9.2 GHz) ESR spectra were recorded on a Varian E-9 spectrometer interfaced to an IBM AT compatible for data collection and signal averaging. The magnetic field was calibrated using a Micro-Now NMR gaussmeter. The proton resonance from an aqueous solution of copper sulfate was used as a calibration standard. The field was calibrated to ±0.01 G. The klystron frequency was measured with a Systron Donner 6420 microwave counter. The klystron frequency is stable to ±10 kHz (0.000 01 GHz). Variable temperature is accomplished using an Air Products Helitran with liquid helium as the coolant.

Ancillary Characterization. Dc magnetic susceptibility data were collected on a SQUID magnetometer at the National Institute of Standards and Technology (NIST) at Boulder, CO. X-ray powder diffraction data was collected on a Siemens automatic powder diffractometer using Cu Kα radiation. FTIR spectra were run on a Perkin-Elmer 1700 spectrometer interfaced to a Spectra Tech IR PLAN 1 microscope. The detector is a mercury–cadmium–telluride (MCT) detector which is cooled with liquid nitrogen. It has a useful range of 7000–700 cm^{-1}. Mass spectroscopic data were obtained on a high-resolution VG 7070 EHF mass spectrometer.

Results

Preliminary Characterization. Dc magnetic susceptibility experiments confirmed that our samples were superconducting below 6 K as reported by Formstone et al.[3] X-ray diffraction data, collecting only {00l} lines, indicate that none of the $SnSe_2$–1%P remains unintercalated. The value of d(001) of 11.43 Å corresponds to an increase of 5.32 Å, consistent with what has previously been observed for cobaltocene intercalation into other layered materials.[5,8] $SnSe_2$–1%P transmits infrared radiation above 700 cm^{-1}, the lower limit of sensitivity of the MCT detector. Upon intercalation of cobaltocene to yield $SnSe_2$–1%$P\{CoCp_2\}_{0.36}$, no infrared radiation is transmitted over the range 7000–700 cm^{-1}. This is consistent with the reported high electrical conductivity of the intercalated phase.[3] Mass spectroscopy of the volatile compounds upon heating under vacuum reveals a strong m/e peak at 189, the parent molecular ion of cobaltocene. The conclusions from this preliminary characterization are that the sample is a superconductor below 6 K, is fully intercalated, is metallic at room temperature, and the cobaltocene remains intact upon intercalation.

Surface Analysis. The XPS spectrum of $SnSe_2$–1%$P\{CoCp_2\}_{0.36}$ recorded at several different times is shown in Figure 1. Several features are immediately apparent. First, the line is a composite one made up of at least two individual lines. Second, the overall shape of the line changes as a function of X-ray exposure time. The low-

(14) Williams, R. H.; Murray, R. B.; Govan, D. W.; Thomas, J. M.; Evans, E. L. *J. Phys. C: Solid State Phys.* 1973, *6*, 3631.

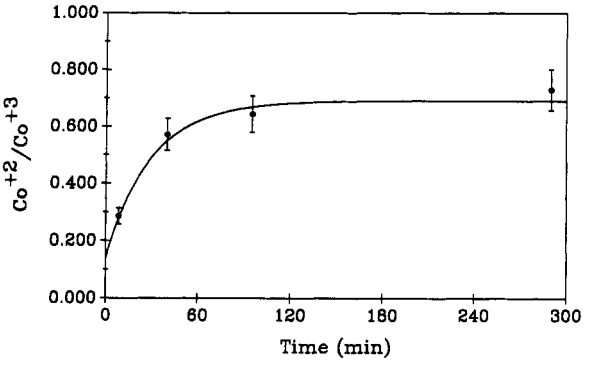

Figure 2. Ratio of Co^{2+}/Co^{3+} as a function of X-ray exposure time. Solid line is a first-order kinetics fit using eq 3; see text.

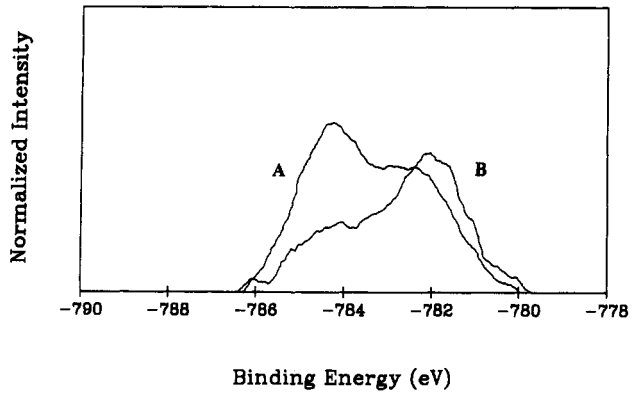

Figure 3. Co $2p_{3/2}$ XPS photoline from $SnSe_2$–1%P{$CoCp_2$}$_{0.36}$ before (A) and after (B) a 5-s, 4-keV argon ion sputter. The effect of the ion sputter is to reduce the high binding energy component of the line shape.

energy line gains intensity as a function of time. This composite nature of the Co $2p_{3/2}$ line has been reported before.[12,15] The assignment, which we adopt, is that the high-energy peak is from Co^{3+} and the low-energy peak from Co^{2+}. It is difficult to determine what the intensity of the Co^{2+} line is at very short exposure times because of the low signal/noise associated with a single XPS scan. ESR experiments (see below) suggest that the concentration of Co^{2+} is low, but not zero. A plot of the intensity of the Co^{2+} peak with respect to the Co^{3+} peak (filled circles) is shown in Figure 2.

The effect of a 4-keV Ar^+ sputter (5 s) can be seen in Figure 3. The high-energy peak (Co^{3+}) is effected much more so than the low-energy peak (Co^{2+}). In Figure 3, the spectrum shown before the sputtering is the result of several hours of X-ray irradiation. The spectrum displayed after sputtering has been exposed for less than 10 min. It is not clear at this time whether Co^{3+} species are being sputtered off the surface or whether they are being reduced to Co^{2+} (or lower).

The amount of cobaltocene intercalated into the $SnSe_2$–1%P lattice was determined from the integrated XPS photolines from Sn and Co. The entire Co $2p_{3/2}$ profile (after 300 min of exposure time) was integrated, and therefore all of the cobalt present has been assigned to either cobaltocene (Co^{2+}) or cobaltocenium (Co^{3+}). No allowance was made for decomposition products containing cobalt.

Electron Spin Resonance. ESR spectra of $SnSe_2$–1%P{$CoCp_2$}$_{0.36}$ for two orientations differing by 90° are shown in Figures 4 and 5. The spectrum in Figure 4

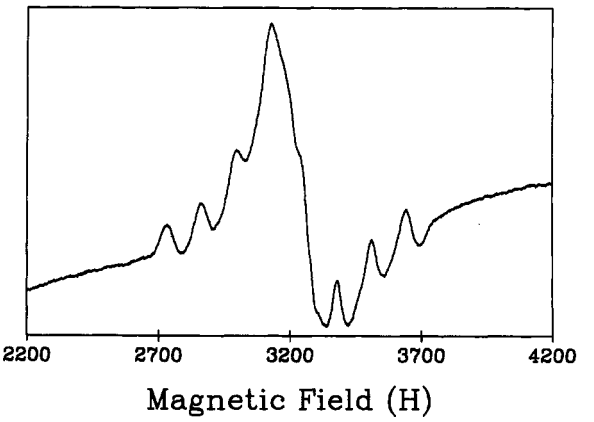

Figure 4. X-band ESR spectrum of $SnSe_2$–1%P{$CoCp_2$}$_{0.36}$ at 5 K. Sample is oriented to maximize the hyperfine resolution. Spectrum is the sum of 49 scans, 1 min/scan.

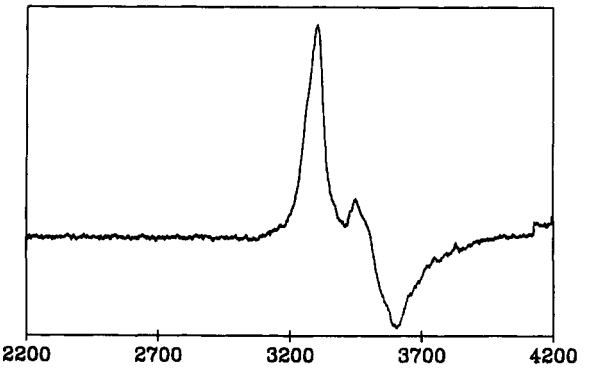

Figure 5. X-band ESR spectrum of $SnSe_2$–1%P{$CoCp_2$}$_{0.36}$ at 5 K. Sample is rotated 90° with respect to the spectrum shown in Figure 4. Spectrum is the sum of 4 scans, 1 min/scan.

Table I. ESR Spin Hamiltonian Parameters for $SnSe_2$–1%P{$CoCp_2$}$_{0.36}$

g_{zz} = 2.047	A_{zz} = 186 MHz
g_{yy} = 1.9[a]	A_{yy} = 70 MHz[a]
g_{xx} = 1.8[a]	A_{xx} = 100 MHz[a]

[a] Estimated.

is the result of signal averaging 49 scans, and the spectrum in Figure 5 was the result of 4 scans. The sweep time was 1 min/scan, the modulation amplitude was 10 G peak-to-peak, the microwave power was 2 mW, and the klystron frequency was 9.213 24 ± 0.000 01 GHz. The spectra were analyzed using a spin Hamiltonian appropriate for $S = {}^1/_2$, $I = {}^7/_2$:[16]

$$\hat{H} = \beta \mathbf{H}\cdot\mathbf{g}\cdot\mathbf{S} + \mathbf{I}\cdot\mathbf{A}\cdot\mathbf{S} \qquad (1)$$

where the symbols have their usual meaning. Resolved hyperfine is seen only in Figure 4, which corresponds to the C_5 molecular symmetry axis of cobaltocene being parallel to the applied magnetic field, H.[17] Hence this spectrum is referred to as the parallel spectrum or the g_{zz} spectrum. Perpendicular to this orientation, Figure 5, one can see that the other two g's, g_{xx} and g_{yy}, are not quite resolved. The hyperfine splitting, A_{xx} and A_{yy}, for this orientation is also not resolved. The lack of hyperfine resolution makes it difficult to determine a unique set of spin Hamiltonian parameters for eq 1. In the parallel spectrum, the spin Hamiltonian reduces to

$$\hat{H} = g_{zz}\beta H M_S + A_{zz}\hat{S}_{zz}\hat{I}_{zz} + A_{yy}\hat{S}_{yy}\hat{I}_{yy} + A_{xx}\hat{S}_{xx}\hat{I}_{xx} \qquad (2)$$

(15) Formstone, C. A.; FitzGerald, E. T.; Cox, P. A.; O'Hare, D. *Inorg. Chem.* **1990**, *29*, 3860.

(16) Abragam, A.; Bleaney, B. *Electron Paramagnetic Resonance of Transition Metal Ions*; Oxford University: Oxford, 1970; pp 133–178.

(17) Ammeter, J. H.; Swalen, J. D. *J. Chem. Phys.* **1972**, *57*, 678.

where the first two terms are diagonal terms in the 16 × 16 matrix of the Hamiltonian. The last two terms connect states $\langle M_s \pm 1, M_I \pm 1 | M_S, M_I \rangle$. The magnitude of $(A_{xx} - A_{yy})$ affects the position of the resonant lines in the parallel orientation, but determining the individual A_{xx} and A_{yy} with any precision is not possible given the lack of resolved hyperfine structure in the perpendicular orientation. A summary of the spin Hamiltonian parameters is given in Table I. The spectra are consistent with neutral cobaltocene being present in the intercalated material. The signal is quite weak, however, and therefore one would expect the concentration of cobaltocene to be low. Our previous work using $Cd_2P_2S_6$ as the host lattice resulted in cobaltocene ESR spectra several orders of magnitude stronger than the present ones for an equivalent size sample. The dramatic angular dependence of the spectrum indicates that the cobaltocene molecules are at least partially ordered within the $SnSe_2$–1%P host. The mosaic nature of our $SnSe_2$–1%P crystals precludes a determination of the cobaltocene orientation with respect to the sulfur layers. The spectra were recorded at 5 ± 1 K. From the low-field microwave absorption (LFMA) we conclude that the sample was in the superconducting state while the data were collected.[18] Above T_c, the cobaltocene spectra persisted, but at reduced strength. The sample has no ESR spectrum at room temperature.

Discussion

The presence of neutral cobaltocene in $SnSe_2$–1%P$\{CoCp_2\}_{0.36}$ is consistent with the observation of a Co^{2+} peak in the XPS spectrum. Cobaltocenium, $CoCp_2^+$, where the cobalt is formally Co^{3+}, is diamagnetic and hence has no ESR spectrum. The conclusion from the ESR experiments is that neutral cobaltocene is present in $SnSe_2$–1%P$\{CoCp_2\}_{0.36}$ but at a low concentration. While it was not possible to determine the orientation of the neutral cobaltocene with respect to the $SnSe_2$–1%P, it can be stated that the cobaltocene is ordered within the $SnSe_2$–1%P. The lack of hyperfine structure in Figure 5 in consistent with an arrangement such that the C_5 molecular axis of each cobaltocene is perpendicular to the applied magnetic field. Similarly, the lack of intensity in the region of g_{xx} or g_{yy} in Figure 4 in consistent with all the C_5 molecular axes being parallel to the applied magnetic field. It remains unclear whether the spectrum in Figure 4 is due entirely to cobaltocene. One could argue that the spectrum is a composite of a cobaltocene spectrum (providing the eight equally spaced lines) and a broad featureless line at $g = 2$. If this is the case, then this second component also is very anisotropic since it is not observed in the perpendicular spectrum, Figure 5.

From the low signal strength in the spectrum shown in Figures 4 and 5, one can conclude that the amount of neutral cobaltocene is low. This is consistent with the argument that the degree of charge transfer between cobaltocene and a host lattice will depend upon the electron affinity of the host lattice. It is complete for TaS_2, χ = 5.2 eV, and only partial for SnS_2 where χ = 4.2 eV. The χ = 4.35 eV of $SnSe_2$ suggests that charge transfer should be greater than the SnS_2 case and less than or equal to the TaS_2 case. The ESR results are consistent with this postulate. The X-ray photoelectron results are less straightforward.

X-ray photoelectron spectroscopy would appear to be the ideal spectroscopic method for determining the relative amounts of two different oxidation states of a metal incorporated into a lattice. Despite being a surface technique with a sampling depth of only a few angstroms, one can cleave samples in situ and characterize "interior" surfaces which presumably represent the bulk. A more formidable problem is faced when the X-rays actually change the physical or chemical nature of the surface under study. In these cases, short exposure times are required to minimized such effects.

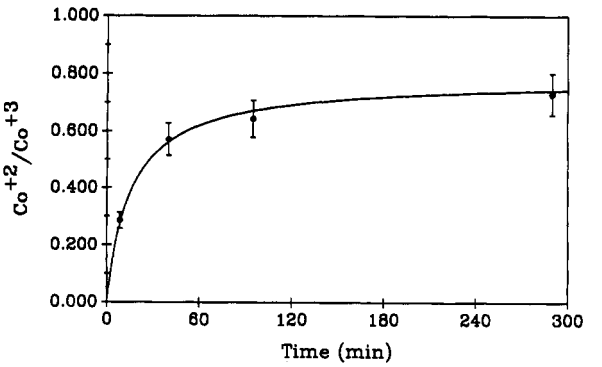

Figure 6. Ratio of Co^{2+}/Co^{3+} as a function of X-ray exposure time. Solid line is a second-order kinetics fit using eq 4; see text.

As the data in Figure 1 clearly show, the Co $2p_{3/2}$ lineshape changes as a function of time. If we adopt the previous assignments for this line, namely, that the high binding energy (more negative) component is from Co^{3+} and the low binding energy component is from Co^{2+}, then after several hours of exposure time it appears that the Co^{2+}/Co^{3+} ratio is 0.7. Combining this ratio with the known total cobalt content allows one to calculate the degree of charge transfer expressed as

$$[Co^{3+}]/([Co^{2+}] + [Co^{3+}])$$

The Co^{2+}/Co^{3+} ratio of 0.7 implies that the degree of charge transfer between the cobaltocene and $SnSe_2$–1%P is lower (60%) than between cobaltocene and SnS_2 (67%). This is contrary to what is expected based on the greater electronegativity of $SnSe_2$. At shorter exposure times, this Co^{2+}/Co^{3+} ratio decreases. The critical question is: what is this ratio at zero exposure time? We have fit the four data points using a nonlinear least-squares fit to both a first- (3) and a second-order (4) kinetics equation:

$$R(t) = R(\infty) - (R(\infty) - R(0))e^{-k_1 t} \quad (3)$$

$$R(t) = R(0) - \left(\frac{R(0)}{R(\infty)} - 1\right)\frac{k_2 t R(\infty)^2}{1 + k_2 t R(\infty)} \quad (4)$$

where $R(\infty)$ is the ratio of Co^{2+}/Co^{3+} as $t \to \infty$, $R(0)$ the same ratio at $t = 0$, k_1 is the first-order rate constant, and k_2 is the second-order rate constant.[19] The result of the first-order fit, assuming a 10% uncertainty in the measured Co^{2+}/Co^{3+} ratio, is $R(\infty) = 0.69 \pm 0.05$, $R(0) = 0.14 \pm 0.08$, and $k_1 = 0.034 \pm 0.017$ min^{-1}. The solid line in Figure 2 is the first-order fit using these parameters and eq 3. Such a fit still suggests a large Co^{2+}/Co^{3+} ratio at $t = 0$ which is inconsistent with the ESR results, although the large uncertainty may account for this difference. The result of the second-order fit is $R(\infty) = 0.78 \pm 0.10$, $R(0) = 0.00 \pm 0.27$, and $k_2 = 0.082 \pm 0.064$ min^{-1}. Figure 6 shows the second-order fit. This time the Co^{2+}/Co^{3+} ratio at $t = 0$ *is* consistent with the ESR results, but again the uncertainty in $R(0)$ is large. To decide which of the two fits is physically reasonable (or whether neither is reasonable),

(18) Cuvier, S.; Puri, M.; Bear, J.; Kevan, L. *Chem. Mater.* **1991**, *3*, 115.

(19) Press, W. H.; Flannery, B. P.; Teukolsky, S. A.; Vetterling, W. T. *Numerical Recipes*; Cambridge University: Cambridge, 1986; p 526.

one must know the processes which are occurring at the surface of the material while it is being irradiated. In either case (first- or second-order process), the Co^{2+}/Co^{3+} ratio extrapolated to $t = 0$ is consistent with $SnSe_2$ having a larger electronegativity with respect to SnS_2.

There are several possible explanations for a different Co^{2+}/Co^{3+} ratio as measured by XPS and ESR. The first is that XPS probes only a few angstroms into the material making a comparison between XPS and ESR data difficult. (ESR typically samples the entire sample volume, see below.) For example, a low concentration of Co^{2+} as determined by ESR would appear as a high Co^{2+} concentration in XPS if the Co^{2+} preferentially reside at the surface of the material. Given that the samples were cleaved in the high-vacuum chamber of the XPS spectrometer to expose fresh interior surfaces, it is not clear that such a surface concentration phenomenon is relevant here. It is possible that the very act of cleaving the material perturbs Co^{2+}/Co^{3+} ratio.

A second explanation for the difference in the Co^{2+}/Co^{3+} ratio as determined by XPS and ESR concerns the penetration depth of microwaves into $SnSe_2$–1%P$\{CoCp_2\}_{0.36}$. As already stated, $SnSe_2$–1%P$\{CoCp_2\}_{0.36}$ is metallic, and therefore there exists a plasma frequency, ω_p, such that for electromagnetic radiation $\omega < \omega_p$, the radiation decays exponentially in the material rather than propagates through it.[20] In Dyson's theory of conduction electron spin resonance (CESR), this effect is manifest through the skin depth, δ, which is the region of the sample where the microwaves have enough amplitude to effect ESR transitions.[21] It should be noted that a typical Dysonian ESR line shape is not observed for any of the temperatures or orientations used in this study. If in $SnSe_2$–1%P$\{CoCp_2\}_{0.36}$ the penetration depth is small, then only a fraction of the total sample volume is subjected to the microwave radiation. Therefore, a correspondingly small fraction of intercalated cobaltocene molecules would undergo ESR transitions and the resultant ESR signal amplitude would not accurately reflect the concentration of paramagnetic molecules within the total sample.

A third possible reason for detecting a small amount of Co^{2+} using ESR is that none of the ESR samples were subjected to X-ray radiation. If most of the Co^{2+} observed in the XPS experiments is the result of radiation processes, then one would not expect similar concentrations to be observed in the nonradiated ESR samples.

(20) Ashcroft, N. W.; Mermin, N. D. *Solid State Physics*; Saunders: Philadelphia, 1976; p 18.
(21) Dyson, F. J. *Phys. Rev.* **1955**, *98*, 349.

Conclusions

We have investigated the time dependence of the Co $2p_{3/2}$ X-ray photoemission line from the intercalation product formed between $SnSe_2$–1%P and cobaltocene, $SnSe_2$–1%P$\{CoCp_2\}_{0.36}$, and have concluded that the line profile changes as a function of X-ray exposure time. This changing line shape suggests that the $SnSe_2$–1%P$\{CoCp_2\}_{0.36}$ undergoes radiation damage and that care must be exercised when using XPS data to determine the relative amounts of Co^{3+} and Co^{2+} in this material. ESR data on $SnSe_2$–1%P$\{CoCp_2\}_{0.36}$ are consistent with the presence of a low concentration of neutral cobaltocene molecules in the intercalated product. The determination of the amount of Co^{2+} in $SnSe_2$–1%P$\{CoCP_2\}_{0.36}$ using XPS depends on how the data is analyzed; a first-order fit suggests a significant concentration of Co^{2+}, and a second-order fit suggests a very low concentration of Co^{2+}. ESR data are consistent with a very low Co^{2+} concentration. A detailed analysis of the magnetic susceptibility of this material might provide valuable insight into the relative amounts of Co^{3+} and Co^{2+} present in this compound.

Acknowledgment. We thank Dr. William Cross of NIST, Boulder, CO, for performing the magnetic susceptibility experiments. We also thank Mr. Mark Engelhard (PNL) for assistance with the XPS experiments. The XPS experiments were supported by the U.S. Department of Energy through Contract No. DE-AC06-76RL0 1830 with Battelle Memorial Institute.

Registry No. $SnSe_2$, 20770-09-6; P, 7723-14-0; cobaltocene, 1277-43-6.